Dyes and Pigments 92 (2012) 1075–1082

Contents lists available at ScienceDirect

Dyes and Pigments

journal homepage: www.elsevier.com/locate/dyepig

Synthesis and characterization of ortho-twisted asymmetric anthracene derivatives for blue organic light emitting diodes (OLEDs)

Min-Gi Shin [a], Seul Ong Kim [a], Hyun Tae Park [b], Sung Jin Park [c], Han Sung Yu [c], Yun-Hi Kim [b,**], Soon-Ki Kwon [a,*]

[a] School of Materials Science & Engineering and ERI, Gyeongsang National University, Gajwa-dong 900, Jinju 660-701, Republic of Korea
[b] Department of Chemistry and RINS, Gyeongsang National University, Jinju 660-701, Republic of Korea
[c] EL Materials Development Division, Duksan Hi-Metal Co. Ltd., Seongnam 463-402, Republic of Korea

ARTICLE INFO

Article history:
Received 4 January 2011
Received in revised form
1 March 2011
Accepted 2 March 2011
Available online 10 March 2011

Keywords:
Blue OLED
Ortho-twisted structure
Asymmetric anthracene
Color purity
Quantum efficiency
Inhibited intermolecular interaction

ABSTRACT

New ortho-twisted asymmetric anthracene derivatives have been synthesized and characterized. The anthracene derivatives show good thermal stability with high glass transition temperatures and a pure blue emission with a narrow full width at half maximum in a film state ($\lambda_{max} = 454$ nm with 71 nm for 2-(2-methylnaphtathalene-1-yl)-9,10-di(naphthalene-2-yl)anthracene and $\lambda_{max} = 445$ nm with 60 nm for 2-(biphenyl-2-yl)-9,10-di(naphthalene-2-yl)anthracene). A multi-layered device using 2-(2-methylnaphtathalene-1-yl)-9,10-di(naphthalene-2-yl)anthracene as an emitting material exhibits a maximum quantum efficiency of 3.61% (power efficiency of 2.15 lm/W, current efficiency of 3.55 cd/A) and blue Commission Internationale de l'Eclairage chromaticity coordinates ($x = 0.15$, $y = 0.13$). A fabricated device using 2-(biphenyl-2-yl)-9,10-di(naphthalene-2-yl)anthracene as an emitting material exhibits a maximum quantum efficiency of 3.7% (power efficiency of 2.11 lm/W, current efficiency of 3.55 cd/A) and a blue Commission Internationale de l'Eclairage chromaticity coordinates ($x = 0.15$, $y = 0.12$).

1. Introduction

Since the first demonstration of electroluminescence from organic fluorescent materials in 1987, organic light-emitting diodes (OLEDs) have been extensively researched because of their potential application to full-color flat-pannel displays [1,2]. Significant progress in material synthesis and device construction have led to the realization of full color as well as white OLEDs with improved efficiencies and lifetimes. Great effort has been made to develop high performance materials with desirable properties and devices with optimized architecture to develop marketable OLEDs [3,4]. While nuerous red [5–7] and green [8–10] materials have been designed, stable, highly efficient, blue-emitting materials have proved more challenging [11–13]. Accordingly, the development of high-performance blue light emitting materials has received attention and many blue materials such as anthracene [14–19], fluorene [12,20], di(styryl)arylene [21,22], tetra(phenyl)pyrene [23–25], tetra(phenyl)silyl [13,16] derivatives have been designed.

Anthracene derivatives have been extensively studied and developed as light-emitting materials in OLEDs owing to their interesting photoluminescence (PL) and electroluminescence (EL) properties [16]. By introducing bulky substituents at the 9,10-positions of anthracene, the molecule becomes highly non-planar due to steric interactions between the substituents and the anthracene core. The fluorescent-quenching interactions caused by intermolecular interactions can thus be suppressed and the non-radiative energy decay can be reduced [26–28].

Recently, our group reported that 2,6,9,10-tetra-substituted anthracene derivatives showed high quantum efficiency and good thermal stability. The introduced substituents at 2,6-positions of anthracene slightly increased the conjugation length, leading to deteriorated color purity, although the efficiency was increased [27].

In this study, we designed new blue emitting materials, composed of 9,10-di(2-naphthyl)anthracene and highly twisted ortho-methylated naphthyl or ortho-phenylated phenyl groups on the 2-position of anthracene. 9,10-Di(2-naphthyl)anthracene (ADN) is one of the best blue host materials, exhibiting a stable and smooth thin film with bright blue emission and efficiency. For improvement of color purity and efficiency, either an ortho-methylated naphthyl or an ortho-phenylated phenyl group was

* Corresponding author. Tel.: +82 55 751 5296; fax: +82 55 753 6311.
** Corresponding author. Tel.: +82 55 751 6016.
E-mail addresses: ykim@gnu.ac.kr (Y.-H. Kim), skwon@gnu.ac.kr (S.-K. Kwon).

0143-7208/$ – see front matter © 2011 Elsevier Ltd. All rights reserved.
doi:10.1016/j.dyepig.2011.03.002

introduced at the 2-position of anthracene. The introduction of ortho-substituents leads to a non-coplanar structure and suppression of the intermolecular interactions. It is anticipated that these new anthracenes will show high efficiency and color purity for blue light emitting materials.

2. Experimental

2.1. Materials

All starting materials were purchased from Aldrich and Strem and were used without further purification.

2.2. Instrument

^{1}H NMR spectra were recorded using a Bruker Avance-300 MHz FT-NMR spectrometer, and chemical shifts were reported in ppm units with tetramethylsilane as internal standard. FT-IR spectra were recorded using a Bruker IFS66 spectrometer. Thermogravimetric analysis (TGA) was performed under nitrogen using a TA instruments 2050 thermogravimetric analyzer. Differential scanning calorimeter (DSC) was conducted under nitrogen using a TA instrument DSC Q10. The both samples were heated at a rate of 10 °C/min. UV-visible spectra and photoluminescence (PL) spectra were measured by Shimadsu UV-1065PC UV-visible spectrophotometer and Perkin Elmer LS50B fluorescence spectrophotometer, respectively. The electrochemical properties of the materials were measured by cyclic voltammetry using an Epsilon C3 in a 0.1 M solution of tetrabutyl ammonium perchlorate in acetonitrile. The organic electroluminescence (EL) devices were fabricated using successive vacuum-deposition of *N*,*N*′-diphen]yl-*N*,*N*′-bis-[4-(phenyl-*m*-tolylamino)phenyl]biphenyl-4,4′-diamine (DNTPD, 700 Å), *N*,*N*′-diphenyl-*N*,*N*′-di(1-naphthyl)-1,1′-biphenyl-4,4′-diamine (NPD, 300 Å), 9.10-di(naphthalene-2-yl)anthracene (ADN):MNAn or BIPAn (3%), tris(8-hydroxyquinoline)aluminum (Alq_3, 400 Å), LiF (5 Å), and Al electrode on top of the ITO glass substrate. The ITO glass with a sheet resistance of about 10 Ω was etched for the anode electrode pattern and cleaned in ultrasonic baths of isopropyl alcohol and acetone. The overlap area of Al and ITO electrodes is about 4 mm^2. A UV zone cleaner (Jeilight Company) was used for further cleaning before vacuum deposition of the organic materials. Vacuum deposition of the organic materials was carried out under a pressure of 2×10^{-7} torr. The deposition rate for organic materials was about 0.1 nm/s. The evaporation rate and the thickness of the film were measured with a quartz oscillator. OLED performance was studied by measuring the current–voltage–luminescence (*I*–*V*–*L*) characteristics, EL, and PL spectra at room temperature. *I*–*V*–*L* characteristics and CIE color coordinates were measured with a Keithley SMU238 and Spectrascan PR650. EL spectra of the devices were measured utilizing a diode array rapid analyzer system (Professional Scientific Instrument Corp.) Fluorescence spectra of the solutions in chloroform were measured using a spectrofluorimeter (Shimadzu Corp.).

2.2.1. 2-Methyl-1-naphthaleneboronic acid (**1**)

2.5 M n-butyllithium (19.9 mL, 50.0 mmol) was slowly added to 1-bromo-2-methyl naphthalene (10 g, 45.0 mmol) in anhydrous tetrahydrofuran (THF) (100 mL) at −78 °C. The mixture was stirred for 30 min at −40 °C. Triethyl borate (19.8 g, 140.0 mmol) was slowly dropped into the mixture and stirred at room temperature. After 12 h, the reaction was terminated by the addition of HCl (2 N, 100 mL) and extracted with ethyl acetate (300 mL). The crude product was purified by recrystallization with hexane. The white solid product was obtained by purification. Yield: 5.76 g (68.5%); m.p. 126.8 °C, ^{1}H NMR (300 MHz, $CDCl_3$, ppm): $\delta = 2.57$ (s, 3H). 5.06 (s, 2H), 7.31 (d, $J = 8.40$ Hz, 1H), 7.50 ~ 7.40 (m, 2H), 7.84 ~ 7.75 (m, 3H). FT-IR (KBr) (cm^{-1}): 3400 (O–H), 3045 (aromatic C–H), 2990 (aliphatic C–H).

2.2.2. 2-Bromobiphenyl (**2**)

1,2-Dibromobenzene (19.34 g, 82.0 mmol) and phenylboronic acid (5 g, 0.4 mmol) were mixed in THF (50 mL). K_2CO_3 (2 M, 20 mL) was added to the mixture. The mixture was then left under a nitrogen stream for 15 min. Tetrakis(triphenylphosphine)palladium ($Pd(PPh_3)_4$) (0.5 g, 0.4 mmol) was added and the result solution was refluxed for 24 h at 110 °C. Once the reaction was completed, the crude product was quenched with HCl (2 N, 100 mL) aqueous solution. The product was extracted with dichloromethane (300 mL). The crude product was purified by column chromatography with hexane. Colorless oily compound was obtained by purification. EI-MS: *m/z* 231 Yield: 4 g (41.8%); ^{1}H NMR (300 MHz, $CDCl_3$, ppm) $\delta = 7.27–7.21$ (m, 1H), 7.41–7.36 (m, 2H), 7.47–7.43 (m, 5H), 7.72 (d, $J = 7.96$ Hz, 1H). FT-IR (KBr) (cm^{-1}): 3030 (aromatic C–H), 2980 (aliphatic C–H), 1419.

2.2.3. 2-(Biphenyl-2-yl)-4,4,5,5-tetramethyl-1,3,2-dioxaborolane (**3**)

2.5 M n-butyllithium (16.47 mL, 41 mmol) was slowly added to 2-bromo-biphenyl (8.00 g, 34 mmol) in THF (100 mL) at −78 °C. The mixture was stirred for 30 min at −40 °C. 2-Isopropoxy-4,4,5,5,-tetramethyl-[1, 3, 2] dioxaborolane (7.66 g, 41 mmol) was slowly dropped into the mixture and stirred at room temperature. After 12 h, the reaction was terminated by the addition of HCl (2 N, 100 mL) and extracted with ethyl acetate (300 mL). The crude product was purified by recrystallization with hexane. The white solid product was obtained by purification. Yield: 6.5 g (60.1%); ^{1}H NMR (300 MHz, $CDCl_3$, ppm) $\delta = 1.25$ (s, 12H), 7.52–7.35 (m, 8H), 7.77 (d, $J = 7.34$, 1H). FT-IR (KBr) (cm^{-1}): 3020 (aromatic C–H), 2985 (aliphatic C–H).

2.2.4. 2-Bromoanthraquinone (**4**)

2-Aminoanthraquinone (15.00 g, 67.2 mmol) and cupric bromide (33.77 g, 151, 19 mmol) were mixed in CH_3CN (250 mL). Tert-butyl nitrite (33.77 g, 151.19 mmol) was added to the mixture and stirred for 2 h. After the reaction was quenched with water (200 mL), the crude product was filtered and washed with CH_3CN. The crude product was purified by column chromatography with hexane/methylene dichloride (1/1). Yellowish compound was obtained by purification. EI-MS: *m/z* 285 m.p. 206 °C, Yield: 13.35 g (69.2%); ^{1}H NMR (300 MHz, $CDCl_3$, ppm) $\delta = 7.80 \sim 7.86$ (m, 2H), 7.93 (dd, $J = 8.30$ 2.12 Hz, 1H), 8.18 (d, $J = 8.3$ Hz, 1H), 8.28 ~ 8.33 (m, 2H), 8.43 (d, $J = 1.98$ Hz, 1H). FT-IR (KBr) (cm^{-1}): 3075 (aromatic C–H), 1681 (C=O), 2980 (aliphatic C–H).

2.2.5. 2-Bromo-9,10-di(naphthalene-2-yl)anthracene (**5**)

N-butyllithium (35.25 mL, 88 mmol) was dropped into 2-bromonaphthalene (16.59 g, 35 mmol) in THF (100 mL) at −78 °C. After 1 h stirring, 2-bromoanthraquinone (10 g, 35 mmol) was added to the mixture at −40 °C and the mixture was stirred for 12 h aqueous ammonium chloride (2 M, 200 mL) was slowly added to the mixture and extracted with diethyl ether (300 mL). After recrystallization with diethyl ether, the recrystallized solid was added in the mixture of acetic acid (100 mL), potassium iodide (17.4 g, 0.105 mol) and hypophosphite soda (22.23 g, 0.210 mol). After the mixture was stirred for 6 h at 120 °C, the crude product was filtered and washed with water and ethanol. The crude product was purified by column chromatography with hexane. Yellowish compound was obtained by purification. EI-MS: *m/z* 508 Yield: 14 g (78.9%); ^{1}H NMR (300 MHz, $CDCl_3$, ppm) $\delta = 7.38 \sim 7.34$ (m, 3H), 7.69 ~ 7.61 (m, 7H), 7.76 ~ 7.71 (m, 2H), 7.91 (d, $J = 3.15$, 1H), 8.01 ~ 7.94 (m, 4H),

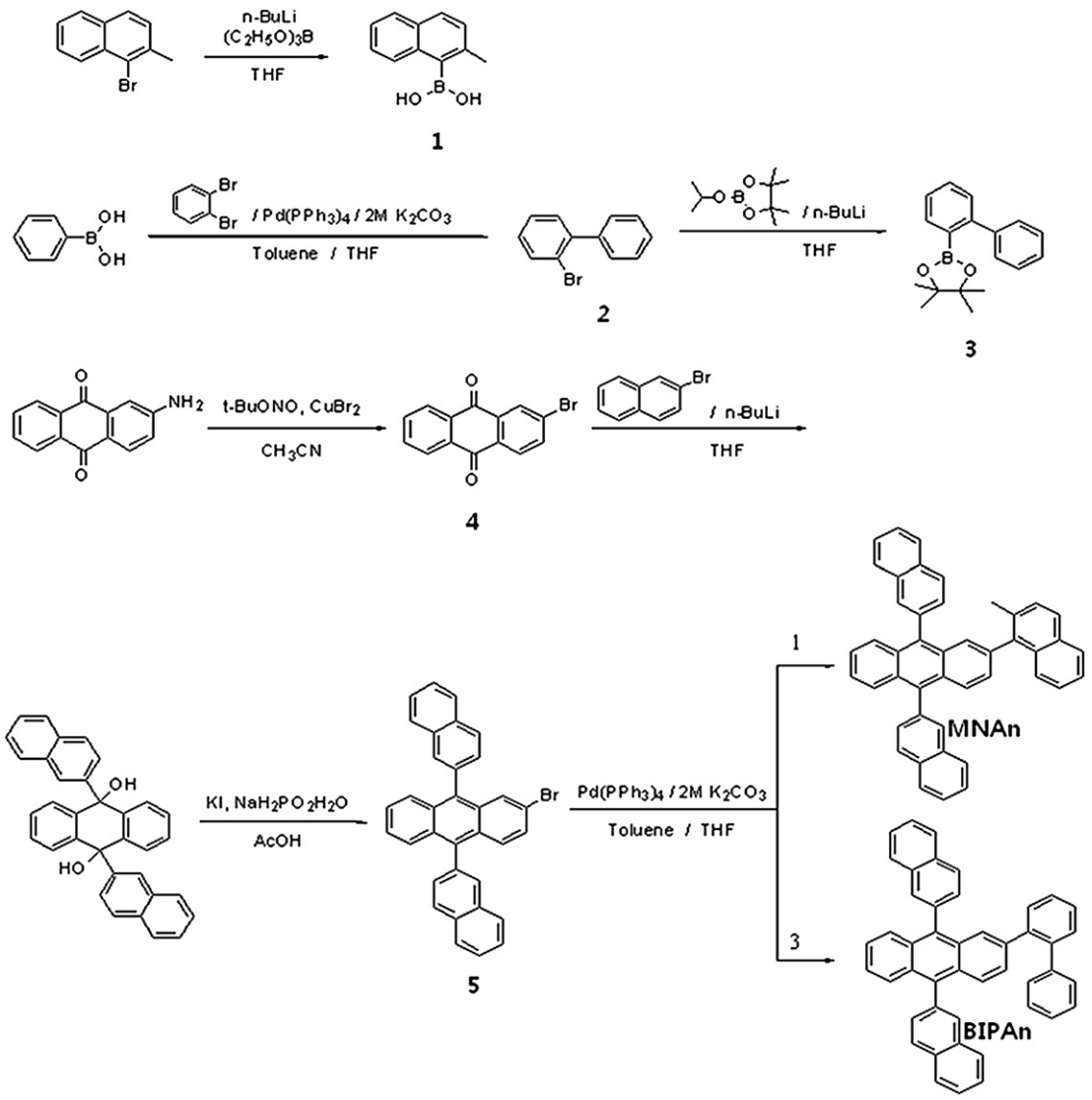

Scheme 1. Synthetic route to MNAn and BIPAn.

8.09 ~ 8.05 (m, 2H), 8.14 ~ 8.10 (m, 2H). FT-IR (KBr) (cm^{-1}): 3043 (aromatic C—H), 2980 (aliphatic C—H), 1572 (C═C).

2.2.6. 2-(2-Methylnaphtathalene-1-yl)-9,10-di(naphthalene-2-yl) anthracene (MNAn)

The product was obtained by the procedure used for the preparation of 2-bromobiphenyl and purified by column chromatography with hexane. The yellowish compound was obtained by sublimation purification. HRMS: calcd. for $C_{45}H_{30}$: 570.2347, found: 570.2353.Yield: 1.96 g (29.17%); ^{1}H NMR (300 MHz, $CDCl_3$, ppm) $\delta = 2.25$ (d, $J = 2.77$, 3H), 7.30 ~ 7.26 (m, 2H), 7.38 ~ 7.31 (m, 4H), 7.57 ~ 7.47 (m, 3H), 7.67 ~ 7.62 (m, 3H), 7.71 ~ 7.70 (m, 1H), 784 ~ 7.73 (m, 5H), 8.02 ~ 7.88 (m, 6H), 8.09 ~ 8.05 (m, 1H), 8.17 ~ 8.12 (m, 2H). FT-IR (KBr) (cm^{-1}): 3030 (aromatic C—H), 2990 (aliphatic C—H).

2.2.7. 2-(Biphenyl-2-yl)-9,10-di(naphthalene-2-yl)anthracene (BIPAn)

2-Bromo-9,10-di(naphthalene-2-yl)anthracene (6 g, 12 mmol) and of 2-(biphenyl-2-yl)-,4,5,5-tetramethyl-1,3,2-dioxaborolane (4.3 g, 15 mmol) was added in the solution of toluene (80 mL), K_2CO_3 (2 M, 40 mL), THF (25 mL) and tetrakis(triphneylphosphine) palladium (0) (0.27 g, 2 mol%). The solution was stirred in N_2 for 24 h at 110 °C. After reaction, the mixture was quenched with HCl (2 N, 100 mL). The crude product was extracted with ethyl ether (300 mL), and the ethyl ether was evaporated. The purification of crude product was carried out by column chromatography with hexane. The yellowish compound was obtained by sublimation purification. HRMS: calcd. for $C_{46}H_{30}$: 582.2347, found: 582.2354. Yield: 5.15 g (75.1%); ^{1}H NMR (300 MHz, $CDCl_3$, ppm) $\delta = 7.03 \sim 7.01$ (m, 2H), 7.15 ~ 7.10 (t, 2H), 7.23 ~ 7.18 (m, 2H), 7.74 (d, $J = 8.26$ Hz, 2H), 7.30 ~ 7.26 (m, 3H), 7.36 ~ 7.34 (m, 3H), 7.42 ~ 7.39 (m, 1H), 7.50 (d, $J = 1.41$ Hz, 1H), 7.69 ~ 7.60 (m, 7H), 7.76 ~ 7.72 (m, 2H), 7.91 ~ 7.88 (m, 1H), 8.06 ~ 8.00 (m, 3H), 8.10 (d, $J = 8.34$ Hz, 1H). FT-IR (KBr) (cm^{-1}): 3050 (aromatic C—H).

3. Results and discussion

The synthetic route for the preparation MNAn and BIPAn is shown in Scheme 1. 2-Bromo-9,10-dinaphthyl anthracene was obtained by nucleophilic addition of 2-lithionaphthalene to 2-bromoanthraquinone followed by an oxidation reaction. MNAn

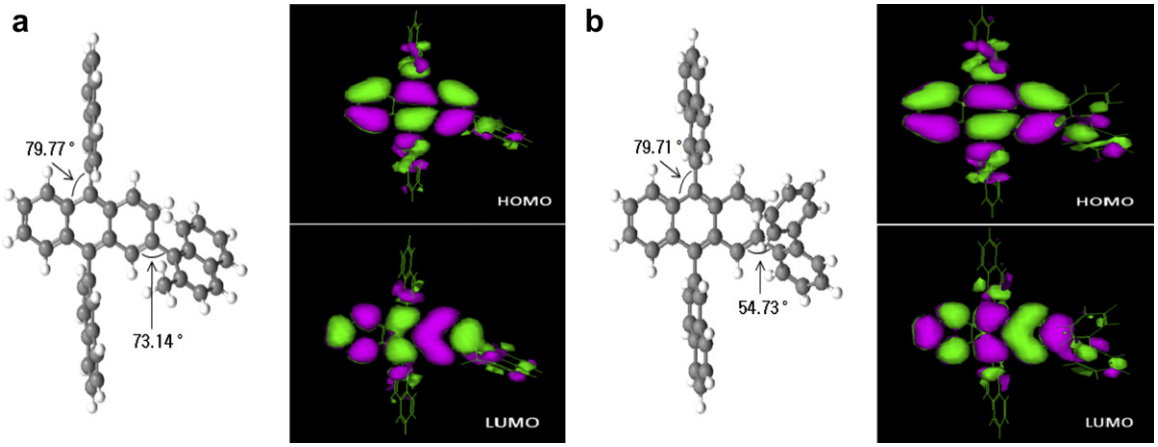

Fig. 1. Calculated stereostructures and the contour plots of HOMO and LUMO energy densities of (a) MNAn and (b) BIPAn.

and BIPAn were synthesized by a Suzuki coupling reaction of 2-bromo-9,10-dinaphthylanthracene with 2-methyl-1-naphthalene boronic acid and 2-(biphenyl-2-yl)-4,4,5,5-tetramethyl-1,3,2-dioxaborolane, respectively. The structures of MNAn and BIPAn were confirmed by ^{1}H-NMR, FT-IR and mass spectroscopy. M^{+} values of the materials were 570.23 m/e and 582.23 m/e, which correspond with their exact mass. Theoretical calculations using the PM3 parameterizations in the HyperChem 5.0 program were carried out to characterize the three dimensional structures and the energy densities of the highest occupied molecular orbital (HOMO) and lowest unoccupied molecular orbital (LUMO) states of each material as shown Fig. 1. Both MNAn and BIPAn are based on anthracene, and have a naphthyl group on the 9,10-position of anthracene, which leads to structural twisting of about 75°∼89°. For MNAn, the introduced ortho-methylated naphthyl at the 2-position of anthracene unit was twisted by about 73.14° due to steric hindrance between the ortho-methyl group of naphthyl and hydrogen of anthracene. BIPAn with an ortho-phenylated

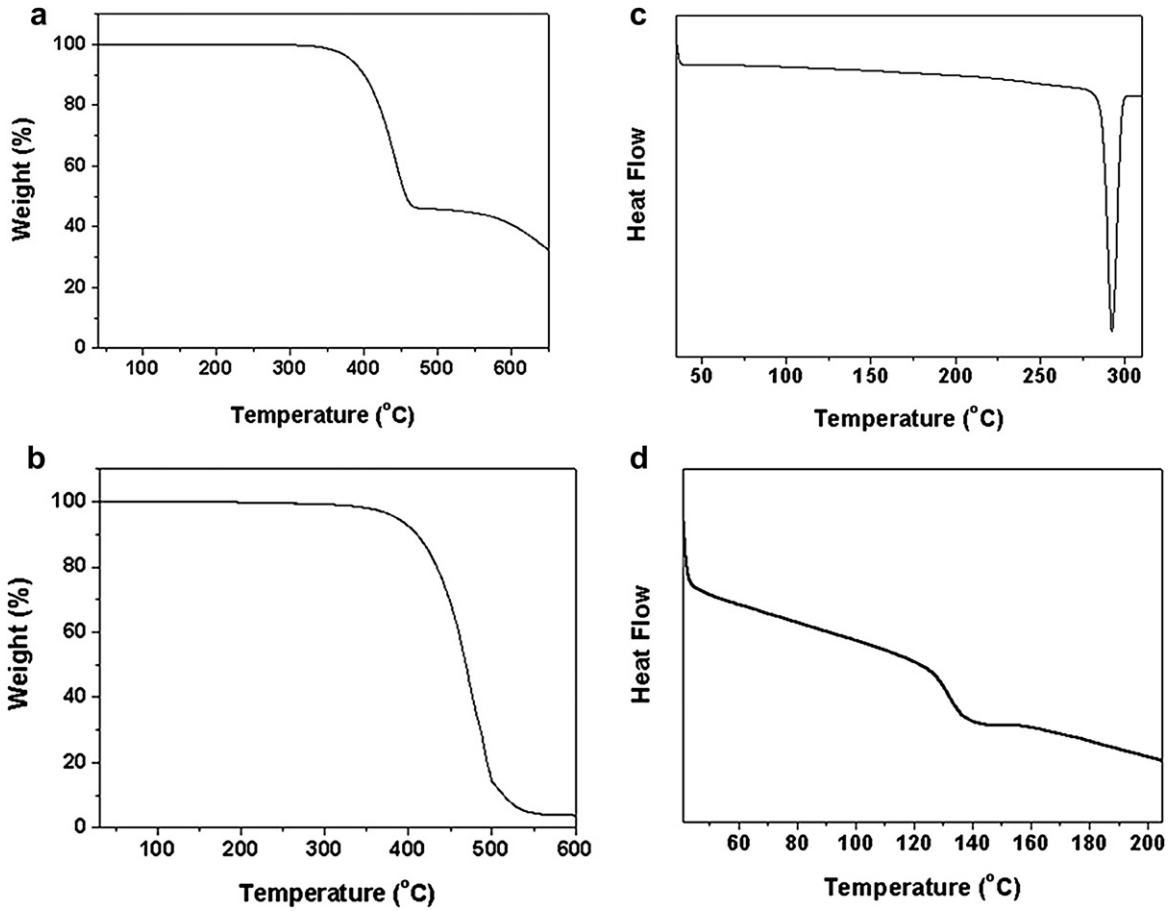

Fig. 2. TGA of (a) MNAn and (b) BIPAn, and DSC of (c) MNAn and (d) BIPAn.

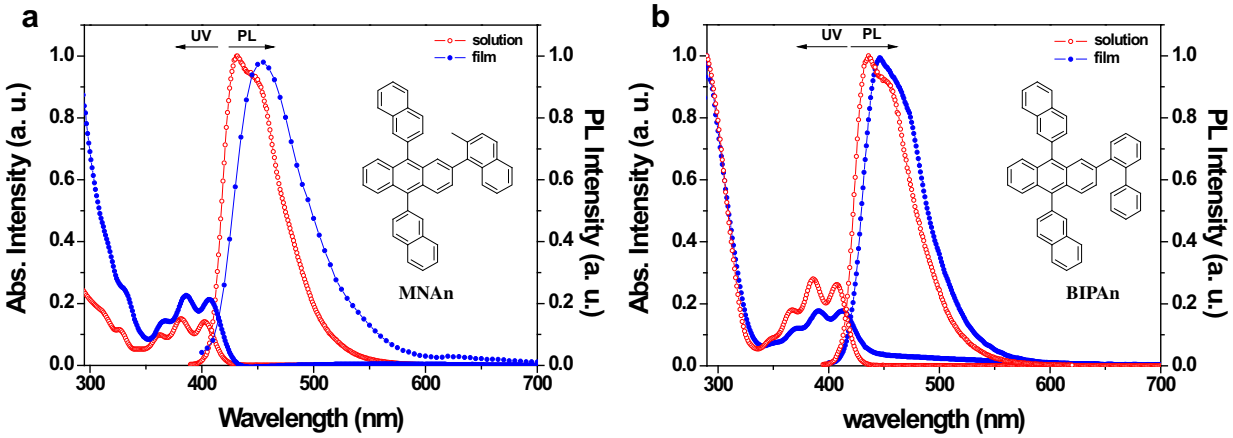

Fig. 3. UV–visible and PL spectrum of (a) MNAn and (b) BIPAn.

Table 1
Electrochemical properties of MNAn and BIPAn.

	Oxidation E_{onset} (V)	HOMO (eV)	UV λ_{max} (nm)	E_g (eV)	LUMO (eV)
MNAn	1.14	−5.58	416	2.98	−2.60
BIPAn	1.15	−5.59	426	2.91	−2.68

*HOMO-LUMO gap (E_g) measured according to the onset of UV absorption ($E_g = 1240/\lambda_{onset}$ eV).
HOMO (eV) measured according to the onset of oxidation (HOMO = 4.44 + E_{onset}: Ferrocene correction = 4.84 − E_{onset} (oxidation of ferrocene) = 4.84 − 0.4 = 4.44).

phenyl was also twisted by about 54.73° (ortho-phenyl anthracene) and 88.29° (biphenyl unit), due to steric hindrance between ortho phenyl and hydrogen of anthracene. The results show that both MNAn and BIPAn have highly twisted non-coplanar structures. These structures lead to improved color purity and high efficiency due to suppressed excimer interaction from intermolecular interaction as well as enhanced morphological stability of the thin film of the OLED device due to disruption of the intermolecular interaction and suppression of the problematic crystallization.

The thermal properties of MNAn and BIPAn were investigated by differential scanning calorimetry (DSC) and thermogravimetric analyses (TGA) (Fig. 2). The decomposition temperatures (T_d: corresponding to 5% weight loss) of MNAn and BIPAn were 382 °C and 386 °C, respectively. BIPAn which contains an ortho-phenylated phenyl group had the glass transition temperature (T_g) of 132 °C. In the case of MNAn, T_g could not be observed while the melting transition temperature (T_m) was observed at 292 °C. As a result, MNAn and BIPAn have good thermal stability despite being relatively low molecular weight organic compounds.

The photophysical properties for MNAn and BIPAn were investigated by UV and PL spectroscopy. Fig. 3 shows the UV-visible absorption and photoluminescence (PL) spectra of MNAn and BIPAn in dilute solution ($CHCl_3$) and in the film. The UV-visible absorption of MNAn and BIPAn show characteristic vibrational patterns of an isolated anthracene group ($\lambda_{max} = 362$, 381 and 402 nm for MNAn, $\lambda_{max} = 364$, 385 and 406 nm for BIPAn). The λ_{max} of the PL spectrum of MNAn in solution was 431 nm while that of film was 454 nm, constituting a 20 nm red-shift from the solution. The full width at half maximum (FWHM) was 57 nm in solution and 71 nm in the film. For BIPAn, the λ_{max} of the PL spectrum in solution and in the film was 435 nm and 445 nm, respectively. The FWHM of BIPAn was 56 nm in solution and 60 nm in the film, which was slightly narrower than that of MNAn. It may be suggested that BIPAn with ortho-phenylated phenyl has higher steric hindrance than MNAn with ortho-methylated phenyl. Because of the twisted structures of MNAn and BIPAn (Fig. 1), a shoulder peak for the excimer does not appear. The twisted structure prevented intermolecular interaction, and consequently luminescence for the excimer could not be observed.

The electrochemical behavior of MNAn and BIPAn were investigated by cyclic voltammetry (CV). The HOMO, LUMO and bandgap are summarized in Table 1. The oxidation peak potentials are high, $E_{ox} = 1.14$ for MNAn and $E_{ox} = 1.15$ for BIPAn (Fig. 4). From the electrochemical data, the HOMO and LUMO were calculated to be −5.58 eV and −2.98 eV for MNAn and −5.59 eV and −2.73 eV for BIPAn, respectively. The energy bandgaps of MNAn and BIPAn are as

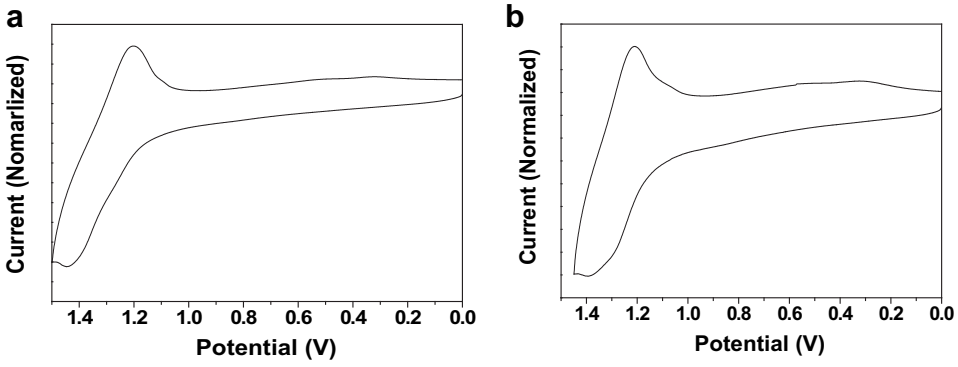

Fig. 4. Cyclic voltammograms of (a) MNAn and (b) BIPAn.

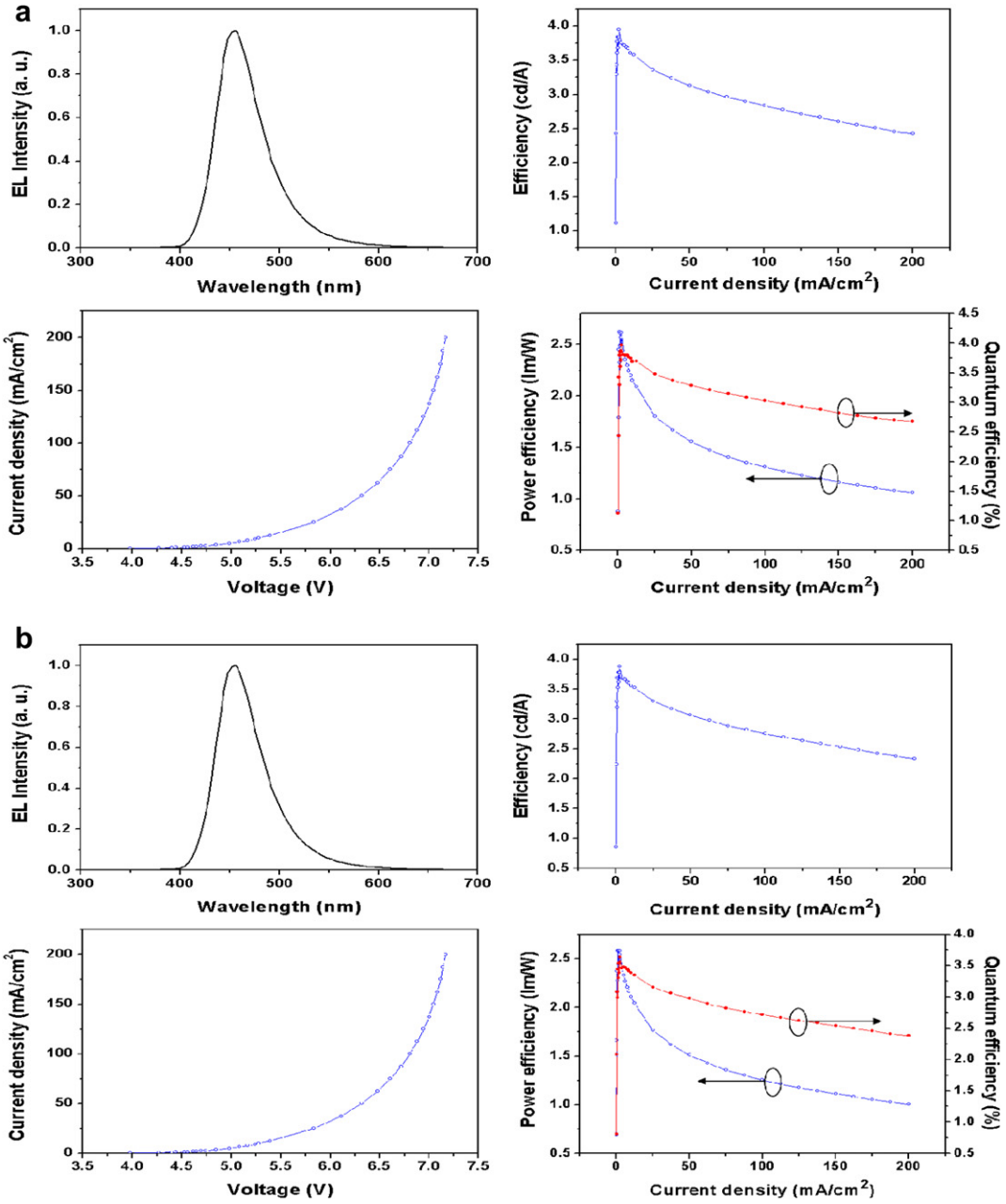

Fig. 5. EL characteristics of (a) MNAn (b) BIPAn as dopant. Device structures: ITO/DNTPD(700 Å)/NPD(300 Å)/ADN:Dopant(3%)/Alq_3(400 Å)/Lif((5 Å)/Al.

wide as 2.98 eV and 2.91 eV, respectively. MNAn and BIPAn are expected to show high efficiency as blue light emitting materials if used as blue dopant materials with the common host ADN (9,10-dinaphthylanthracene), which has a HOMO level of −5.88 eV and a LUMO level of −2.6 eV.

To study the electroluminescence properties of MNAn and BIPAn, multilayer devices with the configuration of ITO/*N*,*N*′-diphenyl-*N*,*N*′-bis-[4-(phenyl-*m*-tolylamino)phenyl]biphenyl-4,4′-diamine (DNTPD, 70 nm)/*N*,*N*′-diphenyl-*N*,*N*′-di(1-naphthyl)-1,1′-biphenyl-4,4′-diamine (α-NPD, 30 nm)/(ADN host/MNAn or BIPAn 3%, 20 nm)/Alq_3 (40 nm)/LiF/Al were fabricated, and ITO and Al were used as an anode and cathode respectively. The stack of the organic layers consists of DNTPD as the hole injection layer, α-NPD as the hole-transport layer, ADN doped with MNAn or BIPAn (3%) as the emitter, Alq_3 as the electron-transport layer, and LiF as the electron-injection layer. In this study, ADN was used as a host for blue-emitting electroluminescence devices. The threshold voltage for luminescence is about 4 ∼ 4.5 V. Fig. 5a and b shows the current density-efficiency curve of the device incorporating MNAn and BIPAn, respectively. The device using MNAn showed a maximum current efficiency of 3.55 cd/A, maximum luminance efficiency of 2.11 lm/W, and maximum external quantum efficiency of 3.38%. The device using BIPAn also showed a maximum current efficiency of 3.61 cd/A, maximum luminance efficiency of 2.15 lm/W, and maximum quantum efficiency of 3.70%. The CIE color chromaticity of the device using MNAn was ($x = 0.15$, $y = 0.13$). The CIE color chromaticity of the device using BIPAn was ($x = 0.15$, $y = 0.12$). The ortho-twisted MNAn and BIPAn showed similar high efficiency as well as similar good color purity. Hypothetical band diagrams of the EL devices are depicted in Fig. 6. The HOMO of MNAn and BIPAn are

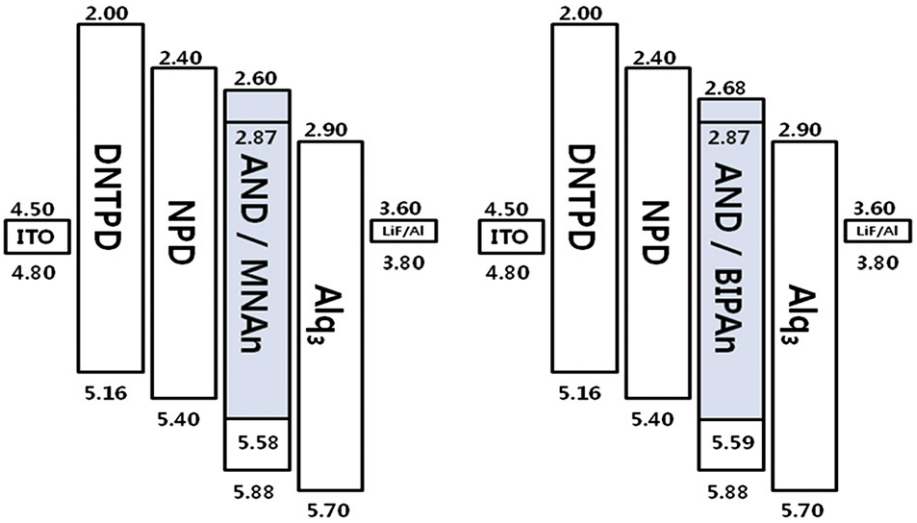

Fig. 6. Energy diagrams of (a) MNAn and (b) BIPAn. (b), (c) and (d) are different structures from (a) about MNAn. Device structures of (a) and (b) are ITO/DNTPD, 70 nm/NPD, 30 nm/(ADN/MNAn or BIPAn 3%, 20 nm)/Alq_3, 40 nm/LiF/Al.

Table 2
EL characteristics of MNAn and BIPAn.

Dopant	Host	λ_{max} (nm)	Current efficiency 10 mA/cm^2 (cd/A)	Power efficiency 10 mA/cm^2 (lm/W)	External quantum efficiency (%)	CIE (x, y)
MNAn	ADN	456	3.55	2.11	3.38	0.15, 0.13
BIPAn	ADN	456	3.61	2.15	3.70	0.15, 0.12

5.58 eV and 5.59 eV, respectively, the HOMO of ADN and NPD are 5.88 eV and 5.4 eV. The hole injection barrier is 0.48 eV from the NPD to the ADN host. In contrast, the barrier for electron transport at the LUMO of ADN/Alq_3 interface is 0.03 eV. Therefore, it is suggested that the electron injection barrier is lower than that of hole injection barrier. Thus, the recombination zone of devices is around the interface NPD and EML. The similar device performance and color purity for MNAn and BIPAN can be explained by their similar energy diagram (Table 2). Device optimization using a wider band gap than ADN host will be expected to increase the performance of devices incorporating MNAn and BIPAN, because a wide band gap host may lead to efficient Foster-type energy transfer from host to the MNAn or BIPAn dopant.

4. Conclusion

New blue emitting materials composed of 9,10-di(2-naphthyl) anthracene and highly twisted ortho-methylated naphthyl or ortho-phenylated phenyl on the 2-position of anthracene have been obtained. The theoretical calculation supports that the synthesized materials have non-coplanar structures, which result in high quality thin films, with high thermal stability, color purity and efficiency due to inhibited intermolecular interaction. Multilayer organic EL devices constructed with a configuration of ITO/DNTPD/NPD/(ADN host/MNAn or BIPAn 3%)/Alq_3/LiF showed a maximum current efficiency of 3.55 cd/A (maximum luminance efficiency of 2.11 lm/W and maximum external quantum efficiency of 3.38%) with CIE color chromaticity of ($x = 0.15$, $y = 0.13$) for MNAN and maximum current efficiency 3.61 cd/A (with the maximum luminance efficiency of 2.15 lm/W and maximum quantum efficiency of 3.70%) with CIE color chromaticity of ($x = 0.15$, $y = 0.12$) for BIPAn.

Acknowledgements

This research was financially supported by MKE and KIAT through the Workforce Development Program in Strategic Technology, by Strategic Technology Under Ministry of Knowledge Economy of Korea and by Basic Science Research Program through the National Research Foundation of Korea (NRF) funded by the Ministry of Education, Science and Technology (2010-0015390).

References

[1] Wu MF, Yeh SJ, Chen CT, Murayama H, Tsuboi T, Li WS. The quest of high-performance host materials for electrophosphorescence blue dopants. Advanced Functional Materials 2007;17:1887–95.
[2] Yang B, Kim SK, Xu H, Park YI, Zhang H, Gu C. The origin of the improved efficiency and stability of triphenylamine-substituted anthracene derivatives for OLEDs: a theoretical investigation. ChemPhysChem 2008;9:2601–9.
[3] Zhao Z, Li JH, Lu P, Yang Y. Fluorescent, carrier-trapping dopants for highly efficient single-layer polyfluorene LEDs. Advanced Functional Materials 2007;17:2203–10.
[4] Shih PI, Chuang CY, Chien CH, Diau EW, Shu CF. Highly efficient non-doped blue-light-emitting diodes based on a anthracene derivative end-capped with tetraphenylethylene groups. Advanced Functional Materials 2007;17:3141–6.
[5] Chen CT. Evolution of red drganic light-emitting diodes: materials and devices. Chemistry of Materials 2004;16:4389–400.
[6] Kim YH, Kim HS, Lee KH, Kwon SK, Kim SH. A novel phenothiazine derivative for application in high performance red emitting electroluminescent device. Molecular Crystals and Liquid Crystals 2006;444:257–63.
[7] Jang JW, Park H, Shin MK, Jung SO, Kwon SK, Kim YH. Novel quinoxaline derivatives containing arylaminated aceanthrylene for organicred-light emitting diodes. Dyes and Pigments 2011;88:44–9.
[8] Kang DM, Kang JW, Kim YH, Shin SC, Kim JJ, Kwon SK. Iridium complexes with cyclometalated 2-cycloalkenyl-pyridine ligands as highly efficient emitters for organic light-emitting diodes. Advanced Materials 2008;20:2003–7.
[9] Park YS, Kang JW, Kang DM, Kim YH, Kwon SK, Kim JJ. Efficient, color stable white organic light-emitting diode based on high energy level yellowish-green dopants. Advanced Materials 2008;20:1957–61.
[10] Jung SO, Kim YH, Kwon SK, Oh HY, Yang JH. New hole blocking material for green-emitting phosphorescent organic electroluminescent devices. Organic Electronics 2007;8:349–56.
[11] Hosokawa C, Higashi H, Nakamura H, Kusumoto T. Highly efficient blue electroluminescence from a distrylarylene emitting layer with a new dopant. Applied Physics Letter 1995;67:3853–6.
[12] Chao TC, Lin YT, Yang CY, Hung TS, Chou HC, Wu CC, et al. Highly efficient UV organic light-emitting devices on based on bi(9,9-diarylfluorene)s. Advanced Materials 2005;17:992–5.
[13] Kim JU, Lee HB, Shin JS, Kim YH, Joe YK, Kwon SK. Synthesis and characterization of new blue light emitting material with tetraphenylsilyl. Synthetic Metals 2005;150:27–32.

[14] Park JK, Lee KH, Kang SW, Lee JY, Park JS, Seo JH. Highly efficient blue-emitting materials based on 10-naphthylanthracene derivatives for OLEDs. Organic Electronics 2010;11:905–15.
[15] Kim YH, Shin DC, Kim SH, Yu HS, Chae YS, Kwon SK. Novel blue emitting material with high color purity. Advanced Materials 2001;13:1690–3.
[16] Kim YH, Jung HC, Kim SH, Yang KY, Kwon SK. High-purity-blue and high-efficiency electroluminescence devices based on anthracene. Advanced Functional Materials 2005;17:1799–805.
[17] Park JW, Kim YH, Jang SH, Lee SK, Shin SC, Kwon SK. Efficient and stable blue organic light-emitting diode based on an anthracene derivative. Thin Solid Films 2008;516:8381–5.
[18] Kim YH, Lee SJ, Byeon KN, Kim JS, Shin SC, Kwon SK. Efficient blue light emitting diode by using anthracene derivative with 3,5-diphenylphenyl wings at 9- and 10-position. Bulletin Korean Chemical Society 2007;28:443–4.
[19] Park JW, Kang P, Park H, Oh HY, Kim YH, Kwon SK. Synthesis and properties of blue-light-emitting anthracene derivative with diphenylamino-fluorene. Dyes and Pigments 2010;85:93–8.
[20] Wu CC, Lin YT, Wong KT, Chen RT, Chien YY. Efficient organic blue-light-emitting devices with double confinement on terfluorenes with amibipolar carrier transport properties. Advanced Materials 2004;16:61–4.
[21] Wang S, Oldham WJ, Hugack RA, Bazan GC. Synthesis, morphology, and optical properties of tetrahedral oligo(phenylenevinylene) materials. Journal of American Chemical Society 2000;122:5695–709.
[22] Burrows PE, Gu G, Bulovi V, Shen Z, Forrest SR, Thompson ME. Achieving full-color organic light emitting devices for lightweight, flat-panel displays. IEEE Transactions on Electron Devices 1997;44:1188–203.
[23] Wu KC, Ku PJ, Lin CS, Shin HT, Wu FK, Huang MJ. The photophysical properties of dipyrenylbenzenes and their application as exceedingly efficient blue emitters for electroluminescent devices. Advanced Functional Materials 2008;18:67–75.
[24] Tang C, Liu F, Xia YJ, Lin J, Xie LH, Zhong GY. Fluorene-substituted pyrenes-novel pyrene derivatves as emitters in nondoped blue OLEDs. Organic Electronics 2006;7:155–62.
[25] Sonar P, Soh MS, Cheng YH, Hensssler JT, Sellinger A. 1,3,6,8-Tetrasubstituted pyrenes: solution-processable materials for application in organic electronics. Organic Letters 2010;12:3292–5.
[26] Kim YH, Kwon SK, Yoo DS, Rubner MF, Wrighton MS. A novel, bright blue electroluminescent polymer: a diphenylanthracene derivative. Chemistry of Materials 1997;9:2699–701.
[27] Jo WJ, Kim YH, Zhao QH, Lee KH, Oh HY, Kwon SK, et al. High efficient organic light emitting diodes using new 9,10-diphenylanthracene derivatives containing bulky substituents on 2,6-position. Synthetic Metals 2009;159:1359–64.
[28] So KH, Park HT, Shin SC, Lee SG, Kwon SK, Kim YH. Synthesis and characterixation of new anthracene-based blue host material. Bulletin of The Korean Chemical Society 2009;42:1611–5.